# Discovery of the $B_c(2S)$ and $B_c^*(2S)$ states

Daniel Alejandro Pérez Navarro on behalf of the CMS collaboration
Cinvestav, México

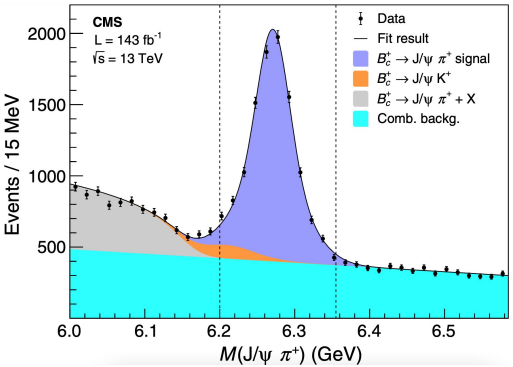


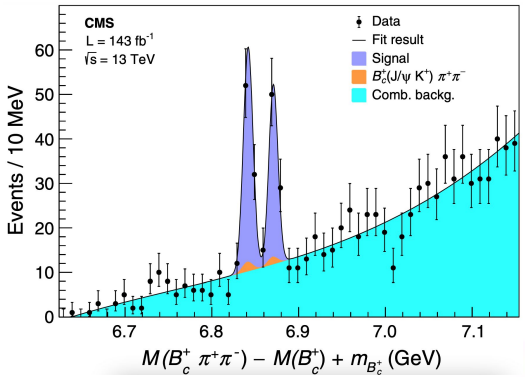

# Outline

- Introduction
- Experimental Apparatus: The CMS Experiment
- Observation of Two Excited $B_C^+$ States
- Measurement of $B_C^+(2S)$ Mass
- Measurement of Cross Section Ratios
- Normalized Invariant Mass Distribution of the Dipion System
- Summary

# Introduction:

- The $B_C$ family consists of charged mesons composed of a beauty quark and a charm antiquark (or vice versa)
- The ground state was discovered in 1998 by the CDF collaboration **[Phys. Rev. Lett. 81, 2432(1998)]**

- The high collision energies and integrated luminosities provided by the LHC have opened the way for new measurements:
  - ATLAS observed a candidate for 2S state at a mass of 6842 ± 4 (stat) ± 5 (sys) MeV using data at 7 and 8 TeV **[Phys. Rev. Lett. 113, 212004 (2014)].**
  - LHCb searched but did not find a significant signature at 8 TeV **[J. High Energy Phys. 01 (2018) 138]**

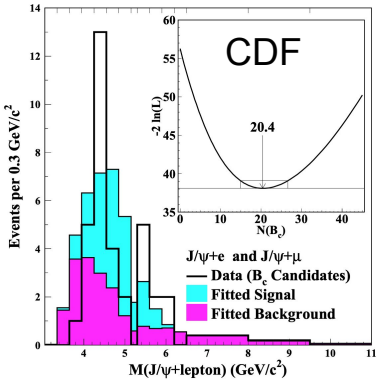


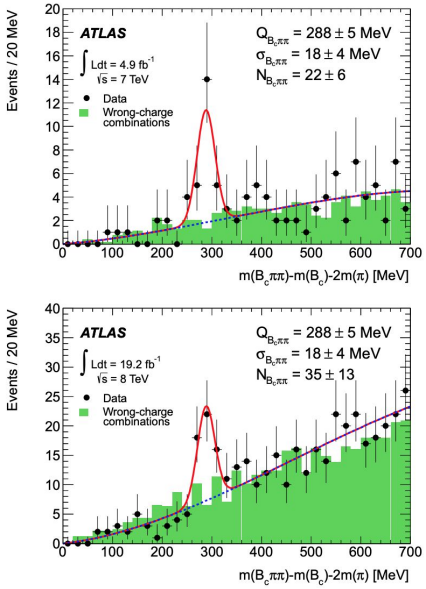


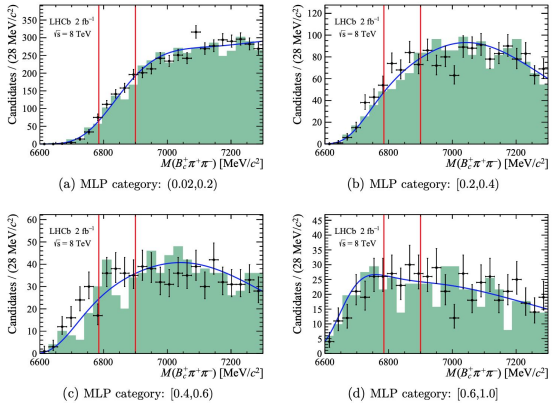

# Introduction:

- In this presentation I will report the results from the CMS collaboration:
  - The observation of well-resolved signals consistent with the $B_C^+(2S)$ and $B_C^{*+}(2S)$ states **(2019)**
  - The first measurement of $B_C^+(2S)$ mass **(2019)**
  - The measurement of $B_C^+(2S)$ to $B_C^+$, $B_C^{*+}(2S)$ to $B_C^+$, and $B_C^{*+}(2S)$ to $B_C^+(2S)$ cross section ratios **(2020)**
  - The invariant mass distributions of the pair of pions emitted in the $B_c^{(*)}(2S)^+ \rightarrow B_c^{(*)+}\pi^+\pi^-$ transition **(2020)**

Results that have been published at:

- Physical Review Letters 122, 132001 (2019)
- Physical Review D 102, 092007 (2020)

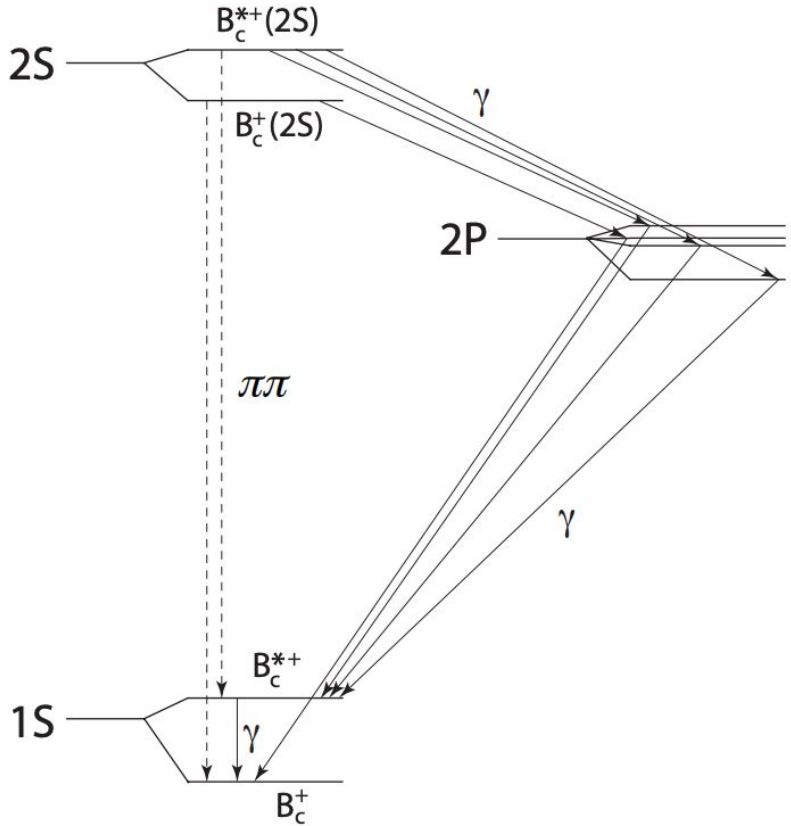


Transitions between the lightest $B_C$ states, with solid and dashed lines indicating the emission of photons and pion pairs, respectively.

E. J. Eichten and C. Quigg, “Mesons with beauty and charm: Spectroscopy”, Phys. Rev. D 49 (1994) 5845, doi:10.1103/PhysRevD.49.5845, arXiv:hep-ph/9402210.

# Introduction

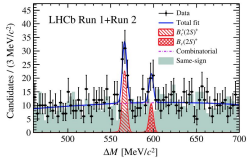


- In 2019 LHCb observed an excited BC+ state using data at 7, 8 and 14 TeV of collision energy
- The mass difference between the $B_C^{*+}$ and $B_C^{+}$ hyperfine partners is predicted to be around 55 MeV, while the corresponding difference between the $B_C^{+}(2S)$ and $B_C^{*+}(2S)$ masses should be around 35 MeV
- The photon involved in the decay of the $B_C^{*+} \rightarrow \gamma B_C^{+}$ is too soft to be detected
- Hence, the $B_C^{*}(2S)^{+}$ peak is visible in the $B_C^{+}\pi^{+}\pi^{-}$ spectrum at:

$$M(B_c(2S)^+) - \Delta M, \text{ where } \Delta M \equiv [M(B_c^{*+}) - M(B_c^+)] - [M(B_c^*(2S)^+) - M(B_c(2S)^+)]$$

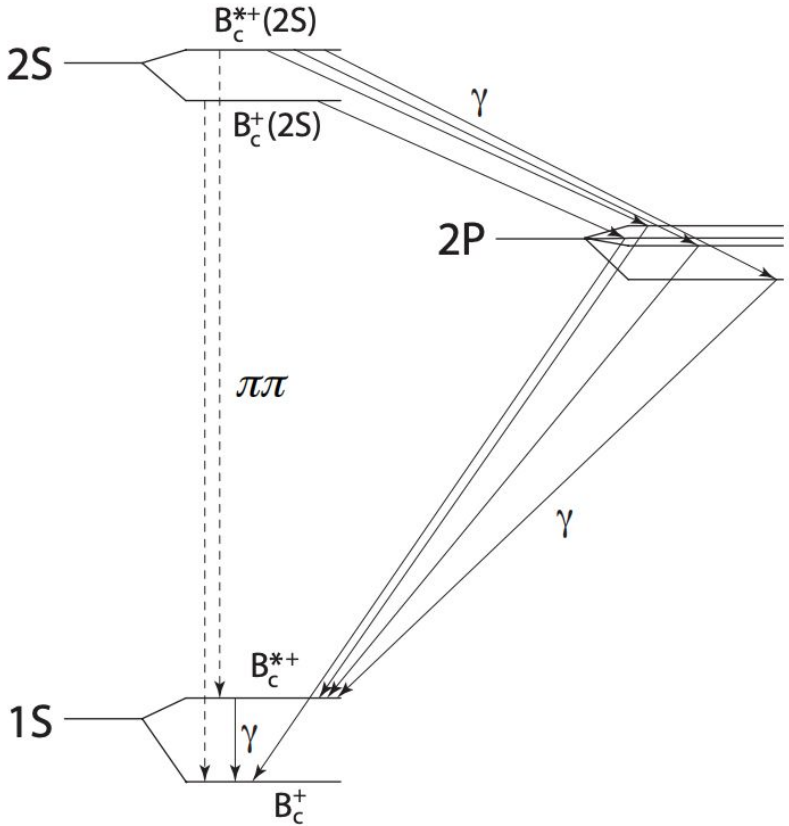


Transitions between the lightest $B_C$ states, with solid and dashed lines indicating the emission of photons and pion pairs, respectively.

E. J. Eichten and C. Quigg, “Mesons with beauty and charm: Spectroscopy”, Phys. Rev. D 49 (1994) 5845, doi:10.1103/PhysRevD.49.5845, arXiv:hep-ph/9402210.

# Experimental Apparatus

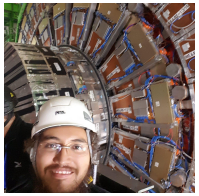

- The central feature of the CMS apparatus is a superconducting solenoid of 6 m internal diameter, providing a magnetic field of 3.8 T.
- Within the solenoid volume are a silicon pixel and strip tracker, a lead tungstate crystal electromagnetic calorimeter, and a brass and scintillator hadron calorimeter, each composed of a barrel and two end cap sections.
- Forward calorimeters extend the pseudorapidity coverage provided by the barrel and end cap detectors.
- Muons are detected in gas-ionization chambers embedded in the steel flux-return yoke outside the solenoid.
- A more detailed description of the CMS detector, together with a definition of the coordinate system used and the relevant kinematic variables, can be found in the reference below.

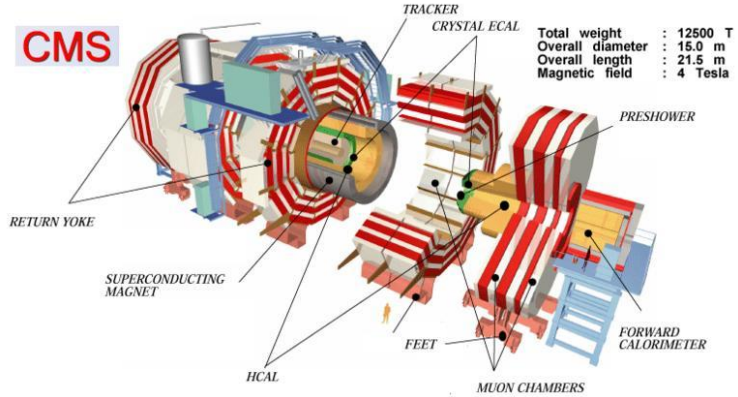


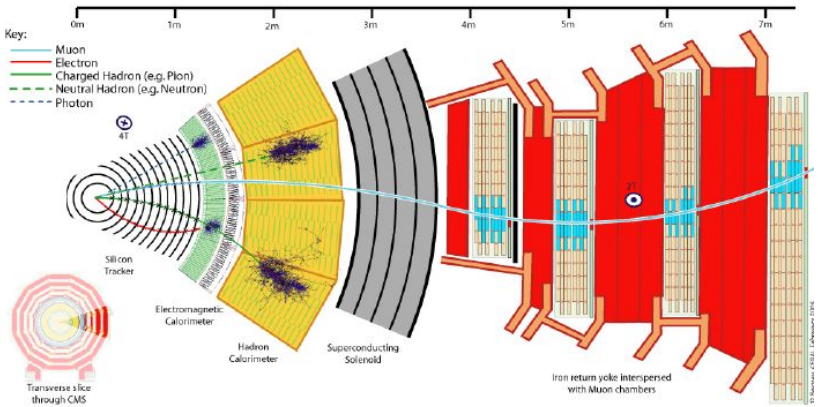


**CMS Collaboration, The CMS experiment at the CERN LHC, J. Instrum. 3, S08004 (2008)**

# Experimental Apparatus

- Muons are measured in pseudorapidity range, |η|<2.4 by the muon subsystem.
- Single muon trigger efficiency over 90%, efficiency to reconstruct and identify muons > 96%
- Matching muons to tracks measured in the silicon tracker results in a relative transverse momentum resolution, for muons with $p_T$ up to 100 GeV, of 1% in the barrel and 3% in the end caps

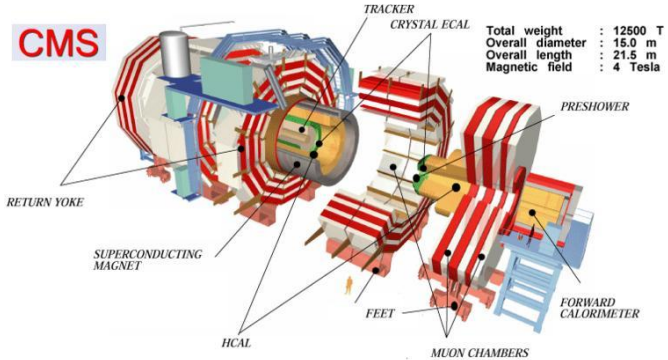


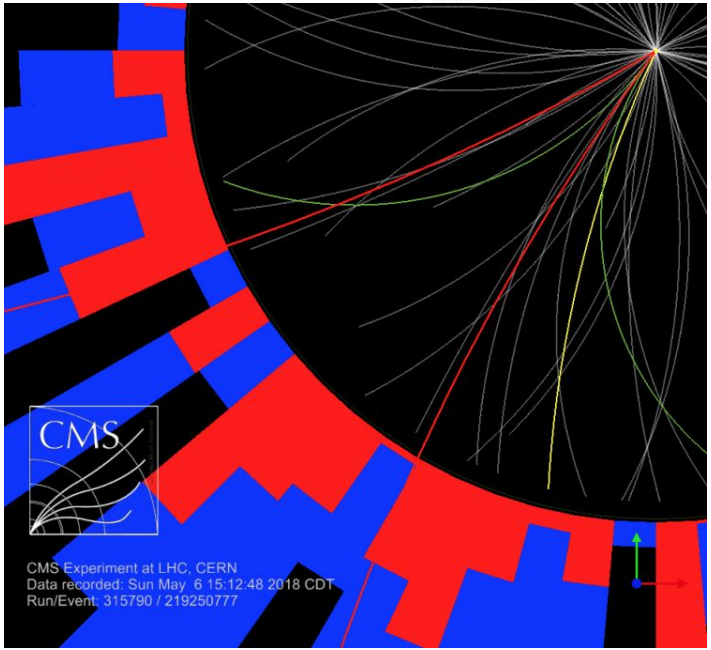

# Experimental Apparatus

Data of 13 TeV pp collisions corresponding to 143 $fb^{-1}$ of integrated luminosity. Measurement in phase space region of $B_C^+$ $p_T$ > 15 GeV, and |η| < 2.4

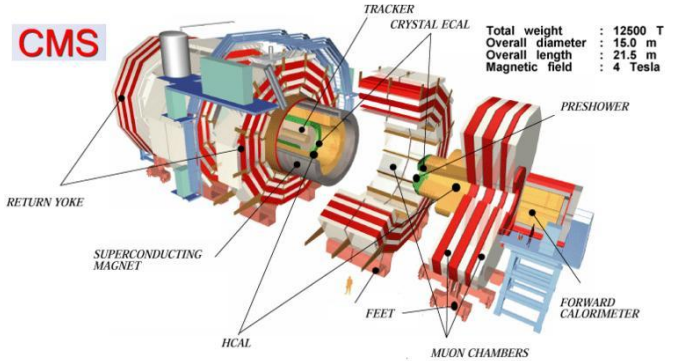


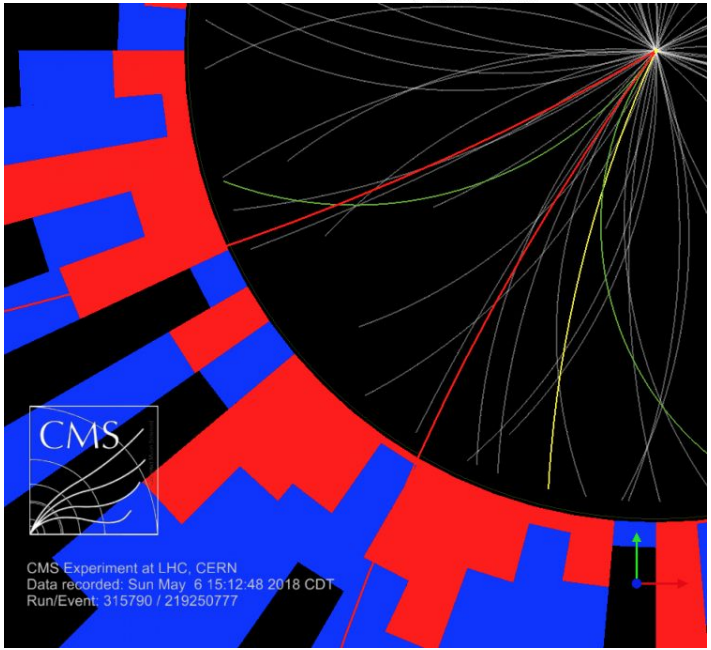


- Dimuon Trigger: 2.8 < m($\mu\mu$) < 3.3 GeV, vertex fit $\chi^2$ probability > 10%, distance of closest approach between muons < 0.5 cm, distance between dimuon vertex and beam axis $L_{xy}$ > three time its uncertainty
- Muons: $p_T$ > 4 GeV, |η|<2.5, $p_T$ must be aligned with $L_{xy}$ by cosθ > 0.9
- Trigger requires a third track: compatible with being produced at dimuon vertex (normalized $\chi^2$ < 10), $p_T$>1.2GeV , |η|<2.5, significance of impact parameter>2

# Observation of two Excited $B_C^+$ States

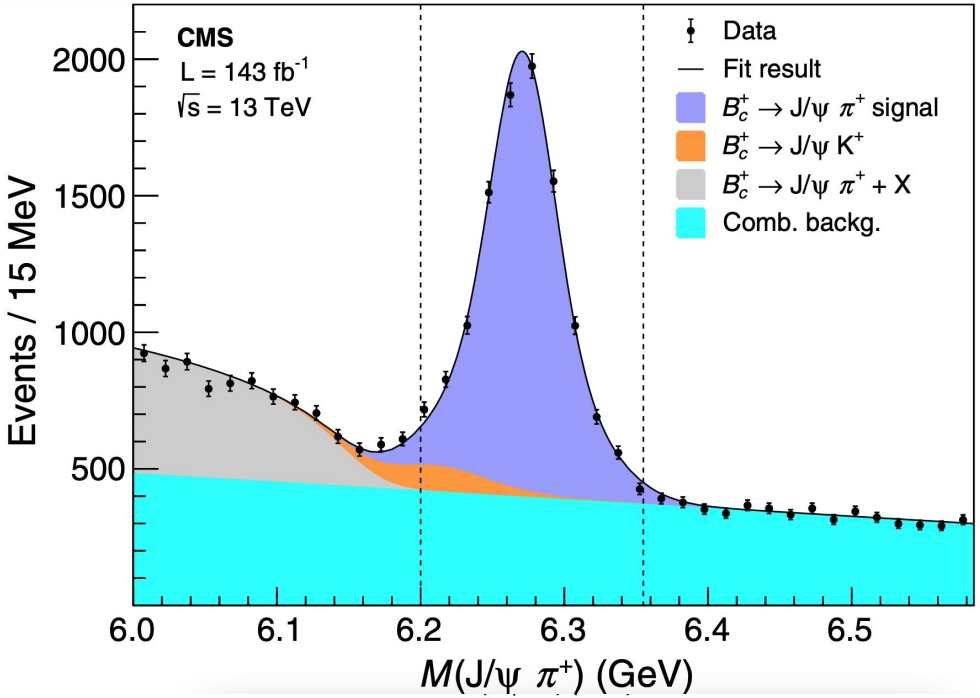


Figure 1: Invariant mass distribution of the $B_c^+ \to J/\psi\,\pi^+$ candidates, after applying all event selection criteria [1]. The fitted contributions are shown by the stacked distributions, the solid line representing their sum. The vertical dashed lines indicate the mass window used to select the $B_c^+$ candidates for the $B_c^{(*)}(2S)^+$ reconstruction.

- The $B_C^+$ candidates are reconstructed by combining the dimuon with a track, assumed to be a pion. This track must have $|\eta| < 2.4$, $p_T > 3.5$ GeV, at least one hit in the pixel layers, at least five hits in the tracker (pixel and strip layers), and an impact parameter in the transverse plane larger than two times its uncertainty
- The $B_C$ candidate is obtained by performing a kinematic fit, imposing a common vertex on the dimuon and pion tracks, and constraining the dimuon invariant mass to be the world average J/ψ mass
- The primary vertex associated with the candidate $B_C$ is selected among all the reconstructed vertices as the one with the smallest angle between the reconstructed $B_C$ momentum and the vector joining the PV with the $B_C$ decay vertex. Studies based on simulation show that the probability of selecting a wrong vertex is less than 1%.

# Observation of two Excited $B_C^+$ States

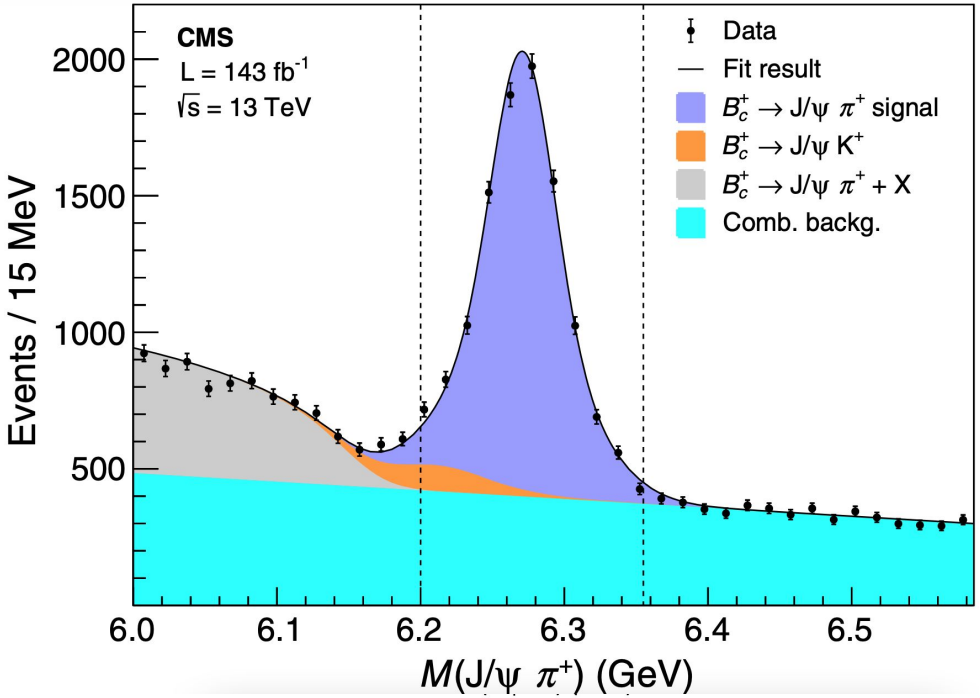


Figure 1: Invariant mass distribution of the $B_c^+ \to J/\psi\,\pi^+$ candidates, after applying all event selection criteria [1]. The fitted contributions are shown by the stacked distributions, the solid line representing their sum. The vertical dashed lines indicate the mass window used to select the $B_c^+$ candidates for the $B_c^{(*)}(2S)^+$ reconstruction.

- $B_C^+$ candidates are required to have $p_T$>15GeV, |y|<2.4, kinematic vertex fit $\chi^2$(prob)>10%, decay length>100$\mu$m.
- Unbinned maximum likelihood fit: signal=double gaussian, background=(a)combinatorial-first order poly,(b)partially reconstructed J/ψ+π+X - generalized ARGUS function, (c)J/ψ+K - fixed shape by simulation studies
- Fitted values: **M($B_C^+$)=6271.1±0.5 MeV**, **$B_C^+$(yield)=7629±255 events**, $\sigma_1$=21MeV, $\sigma_2$= 42 MeV
- $\chi^2$ between binned distribution and the fit function is 35 for 30 degrees of freedom

# Observation of two Excited $B_C^+$ States

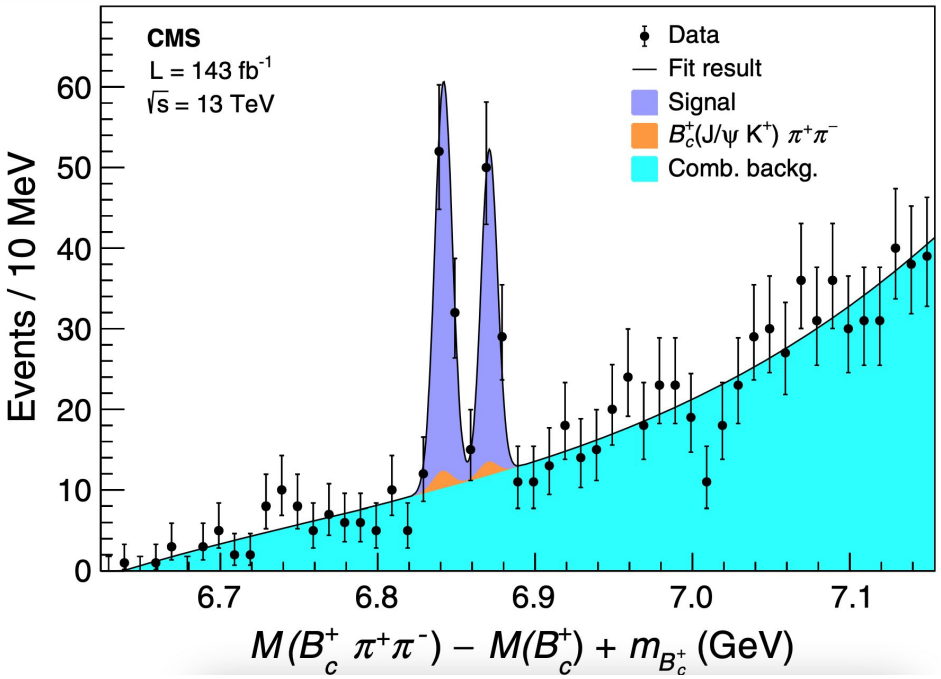


Figure 2: Invariant mass distribution of the $B_c^{(*)}(2S)^+ \to B_c^{(*)+}\pi^+\pi^-$ candidates [1]. The $B_c^*(2S)^+$ corresponds to the lower-mass peak, the $B_c(2S)^+$ to the higher. The fitted contributions are shown by the stacked distributions, the solid line representing their sum.

- $B_C\pi^+\pi^+$ candidates must have |y|<2.4, and vertex kinematic fit $\chi^2$(prob)>10%
- Two signal peaks are fitted with gaussians, a third-order polynomial is used for combinatorial background, and two $B_C^+ \to J/\psi+K$ contributions are fitted to double gaussians with normalization fixed by the ratio of $B_C^+ \to J/\psi+K$ to $B_C^+ \to J/\psi+\pi$ signal yields
- The fit gives **67±10 events** for the **lower-mass** peak and **51±10 for** the **higher**, with a 42/39 $\chi^2$ per degree of freedom
- The mass difference obtained is **ΔM=29.1±1.5 MeV**
- Given the unreconstructed low-energy photon, the $B_C^*(2S)^+$ peak position is at:

$$M\left(B_c(2S)^+\right) - \Delta M, \text{ where } \Delta M \equiv \left[M\left(B_c^{*+}\right) - M\left(B_c^+\right)\right] - \left[M\left(B_c^*(2S)^+\right) - M\left(B_c(2S)^+\right)\right]$$

# Measurement of $B_C^+(2S)$ Mass

- The two states are reconstructed as two well-resolved peaks, separated in mass by

  **29.1 ± 1.5(stat) ± 0.7(syst) MeV**.

- The observation of two peaks, rather than one, is established with a significance of 6.5 standard deviations. This was evaluated with the likelihood-ratio technique confronting the two peaks (ten free parameters) and one-peak (seven free parameters) hypotheses, using asymptotic formulae and accounting for the (dominant) systematic uncertainty in the signal model.
- The mass of the $B_C^+$ (2S) meson is measured to be

  **6871.0 ± 1.2 (stat) ± 0.8 (syst) ± 0.8 ($B_c^+$) MeV**

  where the last term corresponds to the uncertainty in the world-average $B_C^+$ mass

# Measurement of Cross Section Ratios

**Reconstruction Efficiencies**

- Trigger efficiencies cancel in the cross section ratios. Reconstruction efficiencies are evaluated from simulated events
- Efficiencies are computed as the ratio of number of events reconstructed and the number of events generated in the phase-space region $p_T(B_C^+) > 15$ GeV and $|y(B_C^+)| < 2.4$
- Stat. uncertainty reflects the finite size of the simulated samples
- Spread uncertainty reflects the difference between the different data taking periods
- Last column reflects uncertainty in pion reconstruction

$$R^+ \equiv \frac{\sigma(\mathrm{B_c}(2S)^+)}{\sigma(\mathrm{B_c^+})}\mathcal{B}(\mathrm{B_c}(2S)^+ \to \mathrm{B_c^+}\pi^+\pi^-) = \frac{N(\mathrm{B_c}(2S)^+)}{N(\mathrm{B_c^+})}\frac{\epsilon(\mathrm{B_c^+})}{\epsilon(\mathrm{B_c}(2S)^+)},$$

$$R^{*+} \equiv \frac{\sigma(\mathrm{B_c^*}(2S)^+)}{\sigma(\mathrm{B_c^+})}\mathcal{B}(\mathrm{B_c^*}(2S)^+ \to \mathrm{B_c^{*+}}\pi^+\pi^-) = \frac{N(\mathrm{B_c^*}(2S)^+)}{N(\mathrm{B_c^+})}\frac{\epsilon(\mathrm{B_c^+})}{\epsilon(\mathrm{B_c^*}(2S)^+)},$$

$$R^{*+}/R^+ = \frac{\sigma(\mathrm{B_c^*}(2S)^+)}{\sigma(\mathrm{B_c}(2S)^+)}\frac{\mathcal{B}(\mathrm{B_c^*}(2S)^+ \to \mathrm{B_c^{*+}}\pi^+\pi^-)}{\mathcal{B}(\mathrm{B_c}(2S)^+ \to \mathrm{B_c^+}\pi^+\pi^-)} = \frac{N(\mathrm{B_c^*}(2S)^+)}{N(\mathrm{B_c}(2S)^+)}\frac{\epsilon(\mathrm{B_c}(2S)^+)}{\epsilon(\mathrm{B_c^*}(2S)^+)}.$$

Table 1: Ratios of the reconstruction efficiencies relevant for the determination of the $R^+$, $R^{*+}$, and $R^{*+}/R^+$ cross section ratios. The central values are followed by the several uncertainties presented in the text.

| | Central | Stat. | Spread | Pions |
|---|---|---|---|---|
| $\epsilon(\mathrm{B_c}(2S)^+)/\epsilon(\mathrm{B_c^+})$ | 0.196 | 1.1% | 1.8% | 4.2% |
| $\epsilon(\mathrm{B_c^*}(2S)^+)/\epsilon(\mathrm{B_c^+})$ | 0.187 | 1.0% | 1.6% | 4.2% |
| $\epsilon(\mathrm{B_c^*}(2S)^+)/\epsilon(\mathrm{B_c}(2S)^+)$ | 0.955 | 1.4% | 0.9% | — |

$$R^+ = (3.47 \pm 0.63\,(\mathrm{stat}) \pm 0.33\,(\mathrm{syst}))\%,$$
$$R^{*+} = (4.69 \pm 0.71\,(\mathrm{stat}) \pm 0.56\,(\mathrm{syst}))\%, \quad \text{and}$$
$$R^{*+}/R^+ = 1.35 \pm 0.32\,(\mathrm{stat}) \pm 0.09\,(\mathrm{syst}).$$

# Measurement of Cross Section Ratios

- For $B_C^+$: background model is varied to an exponential function, signal model varied to Student's t function
- For $B_C^{(*)}(2S)^+$: background varied to

$$\delta^{\Lambda} \exp(\nu\,\delta), \text{ where } \delta \equiv M(B_c^+\pi^+\pi^-) - q_0$$

signal variation was explored with 2 methods: using one gaussian, and sidebands fitting to background combined with event counting in signal region

- $B_C^+\pi^+\pi^+$ is reconstructed assuming no kinematic correlations between the pions. The assumption is tested by reweighting the simulation to consider (a) an intermediate resonance, and (b) spin dependence
- The analysis is redone by splitting the events into three $B_C^+$ $p_T$ bins and (independently) into three |y| bins
- Bin edges are chosen to have similar uncertainties
- None of the ratios show significant variations, within probed kinematic regions

Table 2: Relative systematic uncertainties (in %) in the cross section ratios, including the $B_c^{(*)}(2S)^+ \to B_c^{(*)+}\pi^+\pi^-$ branching fractions, corresponding to the sources described in the text. The total uncertainty is the sum in quadrature of the individual terms.

| | $R^+$ | $R^{*+}$ | $R^{*+}/R^+$ |
|---|---|---|---|
| $J/\psi\,\pi^+$ fit model | 5.5 | 5.5 | — |
| $B_c^+\pi^+\pi^-$ fit model | 5.9 | 2.9 | 2.9 |
| Efficiencies: statistical uncertainty | 1.1 | 1.0 | 1.4 |
| Efficiencies: spread among years | 1.8 | 1.6 | 0.9 |
| Efficiencies: pion tracking | 4.2 | 4.2 | — |
| Decay kinematics | 1.5 | 6.9 | 4.2 |
| Helicity angle | 1.0 | 6.0 | 3.5 |
| Total | 9.5 | 12.0 | 6.4 |

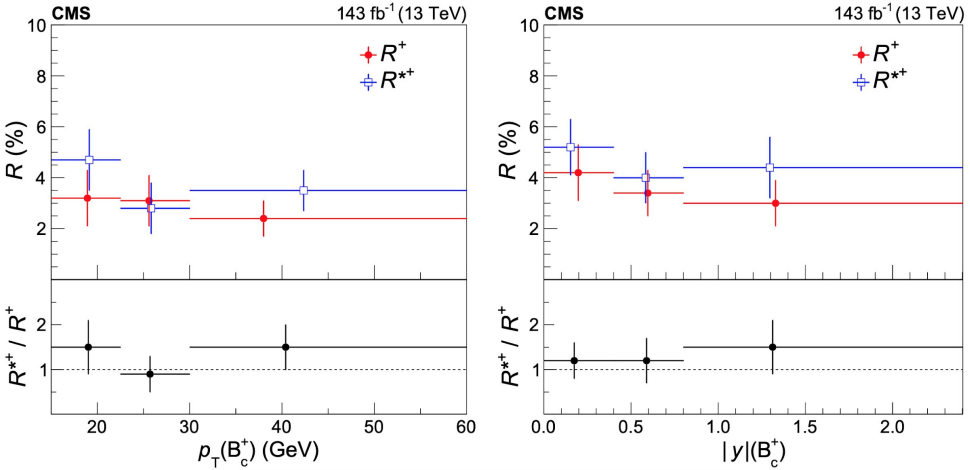


Figure 3: The $R^+$ and $R^{*+}$ (upper), and $R^{*+}/R^+$ (lower) cross section ratios, including the $B_c^{(*)}(2S)^+ \to B_c^{(*)+}\pi^+\pi^-$ branching fractions, as functions of the $B_c^+$ $p_T$ (left) and $|y|$ (right). The horizontal bars show the bin widths. The markers are shown at the average $B_c^+$ $p_T$ or $|y|$ values of the events contributing to each bin, in the background-subtracted distributions, and the vertical bars represent the statistical uncertainties only. The systematic uncertainties are essentially independent of the $B_c^+$ kinematics.

# Normalized Invariant Mass of the Dipion System

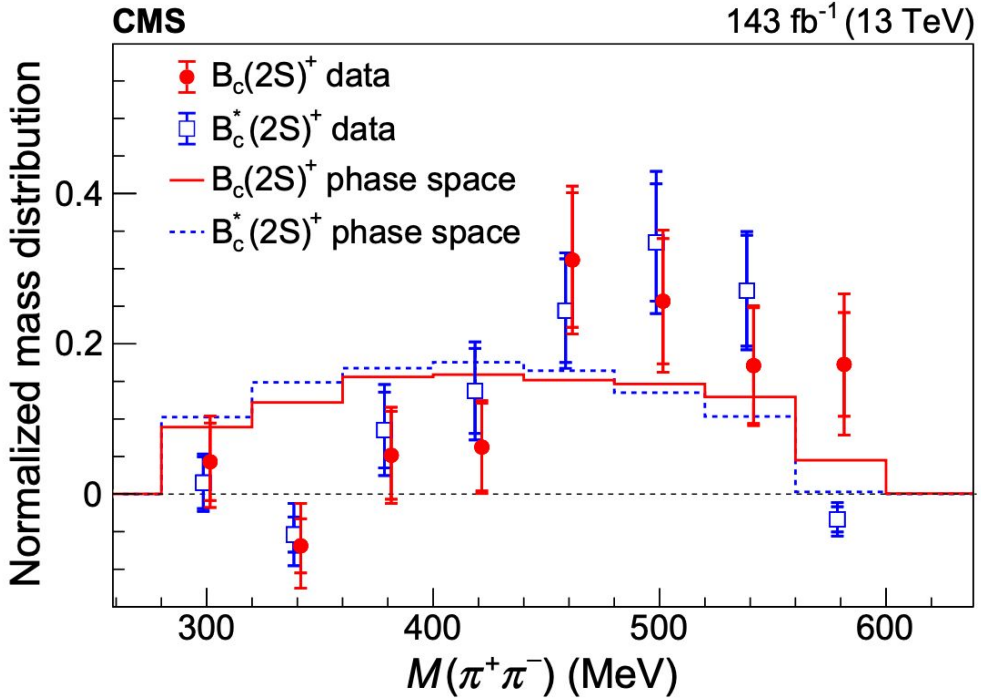


Figure 4: The dipion invariant mass distributions from $B_c^{(*)}(2S)^+ \to B_c^{(*)+}\pi^+\pi^-$ decays in data, normalized to unity. The inner and outer tick marks designate the statistical and total uncertainties, respectively. The lines show the corresponding predictions from phase space simulations.

- As a complement to the cross section ratios, the dipion distribution in the $B_C^+\pi^+\pi^-$ decays may provide relevant information to the production processes of the $B_C^{(*)}(2S)^+$ states
- $B_C^{(*)}(2S)^+$ dipion mass distributions are compatible with each other, and have shapes different from the simulation
- Inner and outer tick marks designate statistical and total uncertainties, respectively

# Summary

- Signals consistent with $B_C^+(2S)$ and $B_C^{*+}(2S)$ have been observed for the first time in the $B_C^+\pi^+\pi^-$ spectrum by CMS
- The analysis uses the entire data set for pp collisions at $\sqrt{s}$ = 13 TeV with 142 $fb^{-1}$ of integrated luminosity
- The two peaks are measured to have a $\Delta M$ 29.1 ± 1.5(stat) ± 0.7(syst) MeV. The $B_C^+$ (2S) is measured to have a mass of 6871.0 ± 1.2(stat) ± 0.8(syst) ± 0.8($B_C^+$) MeV, where the last term corresponds to the uncertainty in the world-average $B_C^+$ mass
- The cross section ratios of $B_C(2S)^+$ to $B_C^+$, $B_C^*(2S)^+$ to $B_C^+$, and $B_C^*(2S)^+$ to $B_C(2S)^+$ have been measured in pp collisions at $\sqrt{s}$ = 13 TeV with a dataset collected by CMS from 2015-2018 corresponding to 143 $fb^{-1}$ of integrated luminosity.
- No significance dependence on transverse momentum or rapidity of the $B_C^+$ mesons is observed for any of the ratios
- The normalized dipion invariant mass distribution for the $B_C^{(*)}(2S)^+ \rightarrow B_C^+\pi^+\pi^-$ is also reported